

# Theoretical and Experimental Investigation of Brake Energy Recovery in Industrial Loads

Nick Papanikolaou<sup>1\*</sup>, John Karatzaferis<sup>2</sup>, Michael Loupis<sup>1</sup>, Emmanuel Tatakis<sup>2</sup>

<sup>1</sup>Department of Electrical Engineering, TEI of Lamia, Lamia, Greece

<sup>2</sup>Laboratory of Electromechanical Energy Conversion (LEMEC), Department of Electrical and Computer Engineering, University of Patras, Patras, Greece

Email: \*npapanikolaou@teilam.gr, jkaratzaferis@ece.upatras.gr, mloupis@teilam.gr, e.c.tatakis@ece.upatras.gr

Received July 16, 2013; revised August 16, 2013; accepted August 24, 2013

Copyright © 2013 Nick Papanikolaou *et al.* This is an open access article distributed under the Creative Commons Attribution License, which permits unrestricted use, distribution, and reproduction in any medium, provided the original work is properly cited.

## ABSTRACT

The issue of calculating the energy saving amount due to regenerative braking implementation in modern AC and DC drives is of great importance, since it will decide whether this feature is cost effective. Although several works have been presented in this subject, they are concentrated on the case of electric vehicles because of the higher energy amounts or the need for more extended autonomy. However, as the increase of the electric energy cost at the Hellenic industrial sector, the need for advanced energy saving techniques emerged in order to cut down operational costs. To this direction, this paper presents a theoretical, simulation and experimental investigation on the quantization of energy recovery due to regenerative braking application in industrial rotating loads. The simulation and the experimental processes evaluate the theoretical calculations, where it is highlighted that annual energy saving may become higher than 10% even for small industrial loads, making the implementation of commercial regenerative braking units rather attractive. Finally, a power electronic conversion scheme is proposed for the storage/exploitation of the recovered energy amount.

**Keywords:** Regenerative Braking; Energy Recovery; Inverters; DC-DC Converters; AC Drives

## 1. Introduction

The purpose of this study is to investigate the possibility of saving energy during braking of industrial loads (rotated by three phase induction motors), as theoretically as experimentally, driven by commercial inverters. The reason why the study focuses on this type of electronic motor drives is due to the fact that it is the most widely used method in the industry, according to a recent analysis of industrial loads in Hellenic Industry (80% of participating businesses use AC Drives) [1].

The following sections include a brief review of the most widely used methods of industrial motor control that are applied by commercial inverters, and a theoretical investigation of the possibility to exploit the braking energy of electric motors driven by commercial inverters, concluding with presenting and evaluating the simulation—experimental results on a commercial inverter.

## 2. Modern Methods of Industrial Voltage Inverter Control

The rapid developments in microcontroller systems over the past ten years gave the impetus to the production of commercial inverters with highly functional features and abundance of possibilities for control [2-4]. These data were presented extensively in a recent analysis of industrial loads in Hellenic Industry [1] and are summarized as follows:

- Wide range of power capacity.
- Soft start, adjustable to small starting current.
- Control of current and voltage output.
- Smooth braking.
- Increased starting torque.
- Automatic or programmable settings.
- Full speed control over a wide range (typically up to 6000 rpm).
- Saving energy.
- Reversible rotation without additional switches.

\*Corresponding author.

- Increased engine protection.
- Silent operation.
- Increased tolerance to background noise and reliability.
- Simple and integrated communications.

The major advantage of using powerful processors to control industrial inverters, to which most of the aforementioned functional characteristics could be attributed, is the application of various vector control methods on three-phase induction motors [5-7]. It is well known from electromechanical systems dynamics theory, that the vector control of three-phase asynchronous motors is based on Park's transformation, *i.e.* the analysis of the motor's electromagnetic values mapped onto a stationary reference system in accordance with the relationship:

$$\begin{bmatrix} i_{qs} \\ i_{ds} \end{bmatrix} = \frac{2}{3} \begin{bmatrix} \sin \theta_f & \sin \left( \theta_f - \frac{2\pi}{3} \right) & \sin \left( \theta_f + \frac{2\pi}{3} \right) \\ \cos \theta_f & \cos \left( \theta_f - \frac{2\pi}{3} \right) & \cos \left( \theta_f + \frac{2\pi}{3} \right) \end{bmatrix} \begin{bmatrix} i_{as} \\ i_{bs} \\ i_{cs} \end{bmatrix} \quad (1)$$

$i_{qs}$ ,  $i_{ds}$ , are the currents in the q, d axes of the static reference system.

$\theta_f$  is the angle of the rotor's interlaced flux,  $\lambda_r$ , relative to the static reference system.

$i_{as}$ ,  $i_{bs}$ ,  $i_{cs}$ , the phase currents of the stator.

If the d axis is aligned with the axis of the interlaced flow  $\lambda_r$  then the current  $i_{ds}$  coincides with excitation current of the asynchronous machine, while the perpendicular vector of current  $i_{qs}$  is the equivalent rotor current (analogous with the separately excited dc machine). Thus, by means of Park's transformation the load current is completely separated from the magnetizing current, rendering the electromagnetic torque fully controllable. This is the basic tool for achieving improved operating characteristics, particularly the smooth acceleration/deceleration (braking) and the increased torque at start-up by 50% - 80%.

Even though the basic vector control method is the direct vector control, the implementation of which requires the existence of a flow sensor to directly measure the induced voltage and a rotor speed sensor, it is worth noting that in modern industrial inverters the following variants of vector control are often adopted:

- **Sensorless Vector Control:** In this case, the flow sensor is not used, and the rotor speed sensor may be absent as well. The vector controller is extracted from the dynamic equations of the induction machine in a synchronous rotating frame of reference, usually aligned to the rotor.
- **Space Vector PWM:** Typically used in high power industrial inverters exceeding 90 kW. The operating principle is based on the fact that the possible states of the switches of a three phase inverter are limited to eight, as the others lead to a short circuit of the input.

Therefore, the reference vector (called space vector) results from the combination of the two adjacent states and the zero states.

### 3. Electric Braking in Modern Industrial Inverters

As already indicated, braking in modern industrial inverters is effectuated via full control of the electromagnetic torque [8-10]. Thus, what is usually set is the deceleration time, which may take typical values of tens of seconds to a few tenths of a second. The process of deceleration is a linear decrease of engine speed so as to avoid impulse load on the axis. Additionally, the inverter user sets the maximum permissible electromagnetic torque during deceleration, for protection against over-current. **Figure 1** illustrates a typical deceleration curve using an industrial inverter. The electromagnetic torque necessary for the implementation of this scheme is the outcome of the torque equation on the motor shaft:

$$-T_e - T'_L = \frac{60J_{ems}}{2\pi} \frac{dn}{dt} \quad (2)$$

$T_e$ , is the absolute value of the electromagnetic torque of the motor.

$T'_L$ , is the absolute value of the load torque reduced on the motor shaft, including any mechanical losses.

$J_{ems}$ , the total moment of inertia of the electric drive system.

$n$ , the rotor speed (rpm).

Since the speed reduction is linear, according to the **Figure 1**, it follows that the rate of change of revolutions can be considered constant and equal to:

$$\frac{dn}{dt} \approx - \frac{n_i}{t_{Br}} \quad (3)$$

$n_i$ , the initial rotor speed at the beginning of braking.

$t_{Br}$ , the set time of deceleration (braking).

Combining Equations (2), (3), we can express the ratio of the mean electromagnetic torque,  $T_{e,avg}$ , to the mean load torque,  $T'_{L,avg}$ , during braking:

$$\frac{T_{e,avg}}{T'_{L,avg}} = \frac{60J_{ems}}{2\pi T'_{L,avg}} \frac{n_i}{t_{Br}} - 1 \quad (4)$$

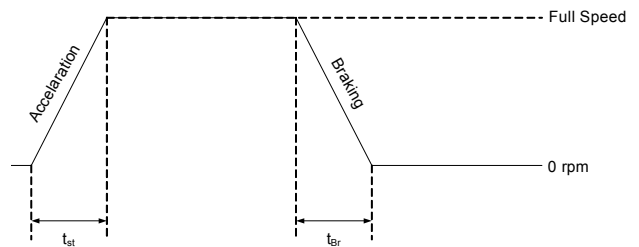


**Figure 1. Typical acceleration—braking curve with an industrial inverter.**

Equation (4) can express qualitatively the percentage of the recoverable braking energy, because evidently the initial kinetic energy of the electric motor system, during braking, is shared upon the work of these two moments. The energy converted into electrical one is expressed by the mean electromagnetic torque whereas the work of the mean load torque is the portion of the kinetic energy consumed by the load and the mechanical losses. Hence:

$$\frac{\Delta E_e}{\Delta E_L} \approx \frac{T_{e,avg}}{T'_{L,avg}} = \frac{60J_{ems}}{2\pi T'_{L,avg}} \frac{n_i}{t_{Br}} - 1 \quad (5)$$

$$E_i = \frac{1}{2} J_{ems} \left( \frac{2\pi n_i}{60} \right)^2 = \Delta E_e + \Delta E_L \quad (6)$$

$E_i$ , is the initial kinetic energy of the electric motor system.

$\Delta E_e$ , is the kinetic energy portion converted into electric energy.

$\Delta E_L$ , is the kinetic energy portion consumed by the load and the mechanical losses.

To what concerns the determination of  $T'_{L,avg}$ , we can safely assume that its value is not affected by the set braking time, because in every case the deceleration follows a linear path. Thus, we can approximate this value by a free braking test ( $T_{e,avg} = 0$ ):

$$0 - T'_{L,avg} = -\frac{60J_{ems}}{2\pi} \frac{n_i}{t_{FR}} \Rightarrow T'_{L,avg} = \frac{60J_{ems}}{2\pi} \frac{n_i}{t_{FR}} \quad (7)$$

Combining Equations (5)-(7) we arrive at the following expression for the braking energy:

$$\frac{\Delta E_e}{\Delta E_L} = \frac{t_{FR}}{t_{Br}} - 1 \quad (8)$$

$$\frac{\Delta E_e}{E_i} = \frac{1}{1 + \left( \frac{t_{FR}}{t_{Br}} - 1 \right)^{-1}} \quad (9)$$

$t_{FR}$ , is the free braking time ( $T_{e,avg} = 0$ ).

**Figure 2** shows the theoretical percentage of the kinetic energy that can be converted into electrical energy during braking of the electric motor system.

We observe that the percentage is significantly increased when the set braking time is substantially reduced relatively to the free braking time. This can be explained in two ways; significant levels of braking energy conversion into electrical can be achieved either if the braking is done with no load on the motor (or at least with reduced load) or by applying a very high electromagnetic torque. Obviously the first case increases time  $t_{FR}$ , while the second case significantly reduces time  $t_{Br}$ . It is shown that the case of no-load brake is beneficial, as in the case of very high electromagnetic torque (100% - 150% of rated torque) the following negative effects take place:

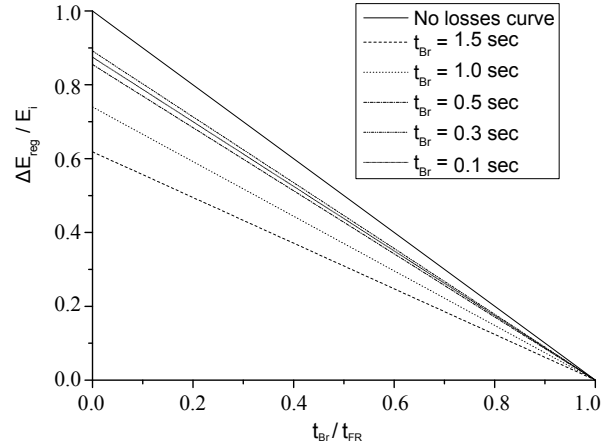


**Figure 2. Kinetic energy recovery potential during braking.**

- Increased electrical copper losses of the motor and conduction losses of the inverter, proportional to the square of to the motor stator current.
- Increased switching losses of the inverter, proportional to the motor stator current.
- In extremely short braking times, intense voltage discharge of the DC link may take place, resulting in excessive electric power consumption from the grid. Additionally, in this case the electric losses of the motor-inverter multiply.
- Deceleration deviates from the desired linearity, due to limiting the set delay time at rates comparable to the time constants of the inverter control.

The conclusion from these observations is that the pursuit of extremely small deceleration times, in order to maximize the percentage of recoverable braking energy, leads to a large increase of electrical losses in the motor and inverter. Thus, the recoverable energy can be significantly reduced, compromising or negating the advantages of electric braking. Finally, the recoverable braking energy results from  $\Delta E_e$  by subtracting the electric losses of the motor and the inverter:

$$\begin{aligned} \Delta E_{reg} &= -\Delta E_{L,inv} - \Delta E_{L,mot} \\ \Rightarrow \frac{\Delta E_{reg}}{E_i} &= \frac{\Delta E_e}{E_i} - \frac{\Delta E_{L,inv} + \Delta E_{L,mot}}{E_i} \end{aligned} \quad (10)$$

$\Delta E_{reg}$ , is the recoverable portion of kinetic energy.

$\Delta E_{L,inv}$ , are the electric inverter losses during braking.

$\Delta E_{L,mot}$ , are the electric motor losses during braking.

As regards both the electrical losses of the inverter and the motor, these can be expressed by the approximate relationship [11,12]:

$$P_{Loss} = P_o + kP^2 \quad (11)$$

$P_{loss}$ , is the power of losses at power level  $P$ .

$P_o$ , is the power of constant losses (irrespective of power level).

$k$ , constant [ $W^{-1}$ ].

Notably, the values of parameters  $k$ ,  $P_o$  are experimentally determined through the analysis of the motor-inverter system losses as a function of operating power. Assuming therefore that the mean power during braking is equal to:

$$P_{Br} = \frac{\Delta E_e}{t_{Br}} \quad (12)$$

We end up by combining Equations (11) and (12), with the following expressions:

$$\frac{\Delta E_{L,inv} + \Delta E_{L,mot}}{E_i} = \frac{\Delta E_e}{E_i} \frac{\Delta E_{L,inv} + \Delta E_{L,mot}}{\Delta E_e} \quad (13)$$

$$\frac{\Delta E_{L,inv} + \Delta E_{L,mot}}{E_i} = \frac{\Delta E_e}{E_i} \frac{P_o + kP_{Br}^2}{P_{Br}} = \frac{\Delta E_e}{E_i} \left( \frac{P_o}{P_{Br}} + kP_{Br} \right) \quad (14)$$

$$E_{reg} = \Delta E_e - \Delta E_{L,inv} - \Delta E_{L,mot} \Rightarrow \frac{\Delta E_{reg}}{E_i} = \frac{\Delta E_e}{E_i} \left( 1 - \frac{P_o}{P_{Br}} - kP_{Br} \right) \quad (15)$$

Equation (15) shows that the energy finally recoverable deviates from the theoretical value of Equation (9), which does not take into account electrical losses. Examples are given in the graphs in **Figure 2**, for parameter values  $k$ ,  $P_o$ , satisfying an efficiency value 85% (for the motor-inverter system) and an initial kinetic energy of 200 Joule (which corresponds to a motor system in the order of 2.5 kW),  $t_{Br}$  being parametric. It is evident from the graphs that an extremely short braking can compromise or reduce the recoverability of energy—similarly to extremely long braking.

Finally, it should be stressed that the recoverable braking energy is usually not harvested in industrial inverters, but otherwise consumed on an ohmic resistor (a part of course is stored in the DC link capacitor). The resistance value is indicated in the technical manuals of industrial inverters and is such as to limit the discharge current,  $I_{ch}$ , to safe levels for the discharge leg. The three-phase inverter circuit including the discharge leg is shown in **Figure 3**. Note that the activation of the discharge leg occurs by detecting overvoltage in the inverter DC link (the activation value varies but is usually in the order of 750 V for three-phase inverters). Nevertheless, the soaring cost of electricity in the Hellenic industrial sector (where the cost increase exceeded 40% the last three years) has constituted particularly attractive the replacement of traditional braking resistors through the adoption of braking energy recovery techniques, such as those studied in this research work.

Consequently the final energy fed into the electric brake circuit and which is recoverable,  $E_{Br}$ , depends on 1) the ohmic resistance of the electric brake circuit (real or equivalent), 2) the capacitance of the DC link capacitor,

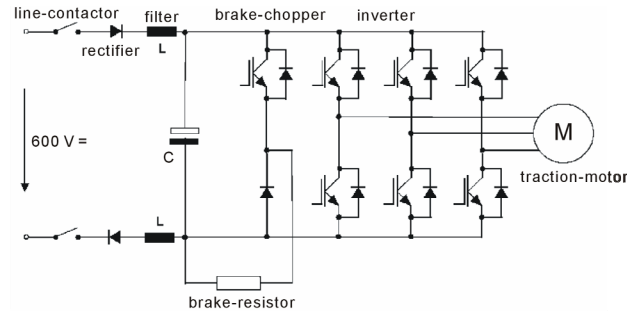


**Figure 3. Industrial inverter circuit with electric break.**

3) from the initial voltage on the DC link, and 4) from the braking time setting,  $t_{Br}$ , according to the relationship:

$$E_{Br} = \frac{1}{2} C_{DC} (V_{DC,i}^2 - V_{DC,f}^2) + \frac{V_{Br,rms}^2}{R_{Br}} t_{Br} \quad (16)$$

$C_{DC}$ , is the capacitance of the DC link capacitor

$V_{DC,i}$ ,  $V_{DC,f}$  are the initial and final voltage values of the DC link capacitor

$V_{Br,rms}$ , is the *rms* value of the voltage which drives the brake resistance during brake

$R_{Br}$ , is the ohmic resistance of the electric brake (real or equivalent)

Comparing Equations (15) and (16) it can be seen that the energy ultimately ending up in the brake resistance can be in the following value ranges:

- $E_{Br} \approx \Delta E_{reg}$ , *i.e.* the value of  $R_{Br}$  is such that as much energy is recovered is driven into the electric brake. Hence the DC link voltage does not fluctuate significantly. This situation is similar to the case of power source matching and thus optimal.
- $E_{Br} < \Delta E_{reg}$ , *i.e.* the value of  $R_{Br}$  is greater than the value corresponding to the matched conditions. In this case the excess recovered energy is stored in the DC link capacitor thereby creating overvoltage. If the overvoltage exceeds the upper threshold voltage (about 750 V - 800 V for industrial inverters), then the brake operation is stopped and the motor decelerates freely.
- $E_{Br} > \Delta E_{reg}$ , *i.e.* the value of  $R_{Br}$  is less than the value corresponding to the matched conditions. In this case the resistance of the electric brake absorbs additional energy from the capacitor of the DC link, creating undervoltage. Undervoltage is apparently covered by the grid via the rectifier unit in the input of the inverter. That is, in this situation the inverter absorbs power from both the load and the grid, similar to the case of the asynchronous motor at brake mode (where slip becomes greater than 100% due to the reverse rotation of the rotor relative to the rotating magnetic field).

The analysis above indicates that the matched resistance,  $R_{Br,match}$ , may result from the combination of Equa-

tions (15), (16), assuming that the variation of the DC link voltage is zero:

$$\left. \begin{aligned} V_{DC,i} = V_{DC,f} = V_{Br,rms} \\ R_{Br,match} = \frac{V_{DC,i}^2}{\Delta E_{reg}} t_{Br} \end{aligned} \right\} \quad (17)$$

At this point it should be noted that the calculation of resistance  $R_{Br,match}$  was made considering that during the braking process the electric brake resistance is constantly connected to the DC link, without the presence of semiconductor switch. If—as in many industrial inverter cases—there is a semiconductor switch that regulates the delivery of energy to the brake, it should remain closed throughout the duration of braking in the case of matching, and therefore the Equation (17) is valid in this case as well.

#### 4. Experimental Results of Measurements upon Industrial Inverter

The following sections present the experimental results from laboratory measurements made upon an industrial inverter. **Figure 4** shows the laboratory electric motor system used in the experimental study, consisting of a three-phase induction motor ( $M_1$ ) driven by an industrial inverter. The mechanical load consists of two DC motors separately excited ( $M_2, M_3$ ) and the consumer used is a

variable resistive load. The presence of two DC motors allows the variation of the moment of inertia of the electric motor system. **Table 1** lists all the technical features of the test system.

To what concerns the experimental procedure, it is consisted of two parts. In the first part, the motor system is consisted of electric motors  $M_1$  and  $M_2$ . There was no electrical load and therefore the motor system simulated a sliding friction mechanical load. The second part involved all three electric motors  $M_1, M_2, M_3$ . Motor  $M_2$  is not stimulated but increases the moment of inertia of the system, while motor  $M_3$  operates as a generator that supplies the electric load. Thereby a mechanical load with a power proportional to the square of the rotational speed is simulated, such as grinding and material polishing machines.

#### 4.1. Section A: Laboratory Measurements with Sliding Friction Load

Experiment data:

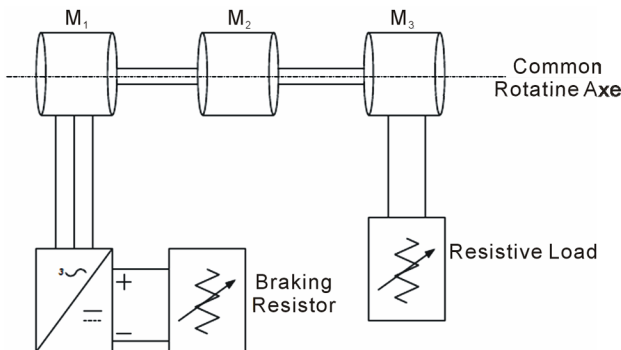
- Total moment of inertia  $J_{ems} = 0.0101 \text{ kgm}^2$ .
- Mechanical load torque  $T'_L = 10\%T_N$  (brake under low load).
- Frequency 50/60 Hz.
- Inverter switching frequency 3 - 6 - 9 - 12 kHz.
- Brake resistance 50  $\Omega$  - 100  $\Omega$  - 200  $\Omega$ .
- Free braking time 4.2 sec/50 Hz, 5.7 sec/60 Hz.

**Table 1. Technical data of the test system components.**

Electric Motors		
$M_1$	$M_2$	$M_3$
<ul style="list-style-type: none"> <li>• Asynchronous three-phase squirrel cage motor 400 V/<math>\Delta</math>, 660 V/Y</li> <li>• 1.5 kW</li> <li>• 3.1 A, 1420 rpm/50 Hz</li> <li>• 2.5 A, 1720 rpm/60 Hz</li> <li>• <math>\cos\phi = 0.8</math> ind</li> <li>• <math>J = 0.0027 \text{ kgm}^2</math></li> </ul>	<ul style="list-style-type: none"> <li>• DC motor separately excited</li> <li>• 220 V, 12 A (Rotor)</li> <li>• 220 V, 0.8 A (Excitation)</li> <li>• 2.2 kW/1500 rpm</li> <li>• <math>J = 0.0074 \text{ kgm}^2</math></li> </ul>	<ul style="list-style-type: none"> <li>• DC motor separately excited</li> <li>• 220 V, 6 A (Rotor)</li> <li>• 220 V, 0.55 A (Excitation)</li> <li>• 1.2 kW/1400 rpm (Generator)</li> <li>• 1.0 kW/1400 rpm (Shunt Motor)</li> <li>• 1.0 kW/1150 rpm (Series Motor)</li> <li>• <math>J = 0.004 \text{ kgm}^2</math></li> </ul>
Industrial inverter	Ohmic resistances	
<ul style="list-style-type: none"> <li>• 3-phase input voltage 400 V/50 - 60 Hz</li> <li>• Maximum power 5.5 kVA</li> <li>• Output voltage 0 - 400 V (phase to phase)</li> <li>• Output frequency 0 - 480 Hz</li> <li>• Efficiency 98% @ 4.5 kW</li> <li>• Sensorless Vector Control</li> <li>• Maximum electromagnetic torque 150%</li> <li>• Electric braking</li> <li>• Braking Semiconductor Switch: No</li> </ul>	<p><b>1) Electric load of variable ohmic resistance</b></p> <ul style="list-style-type: none"> <li>• Maximum power 3.5 kW</li> <li>• 230 <math>V_{rms}</math>/5 A per phase (three independent phases)</li> <li>• <math>\cos\phi = 0.98</math></li> </ul> <p><b>2) Electric brake resistance</b></p> <ul style="list-style-type: none"> <li>• 3 free wiring resistors</li> <li>• 100 Ohm, 500 W per resistor</li> <li>• <math>\cos\phi = 0.98</math></li> </ul>	
Modelling of the electrical losses of the asynchronous motor - industrial inverter system:		
<ul style="list-style-type: none"> <li>• <math>k = 6 \times 10^{-4} \text{ W}^{-1}</math></li> <li>• <math>P_o = 50 \text{ W}</math></li> <li>• Combined Efficiency 83% @ 1.5 kW - 50 Hz</li> </ul>		



(a)



(b)

**Figure 4.** (a) The experimental set-up for measurements—Real laboratory setup; (b) The experimental set-up for measurements—Functional diagram.

Table 2 shows the matching resistance value for 50 Hz and 60 Hz, according to Equation (17), taking into account the electrical losses of the electric motor system according to Figure 2. From the values in Table 2 it is evident that matching is achieved under extremely high values of the electric brake ohmic resistance, mainly due to the power level of the application. Therefore, in every case the ohmic resistance of the electric brake is less than the matching resistance. Hence, according to the theoretical analysis, the energy supplied to the brake resistance is expected to be greater than the recovered energy.

Figures 5-12 confirm this fact, especially for the ohmic resistance of 50 Ohm and for braking times of less than 1.0 sec. The fact that for braking times greater than 1.0 sec the electric brake energy is reduced, can be attributed mainly to a higher energy percentage stored in the DC link capacitor, without causing prohibitive overvoltage—because of the low braking power. On the other hand, reduction of the brake energy is limited in highly dynamic braking (braking times in the order of 0.3 sec) due to excessive increase of power loss in the motor system, in accordance with Equation (15), as the braking

**Table 2.** Matching break resistor value for Section A experiments.

$t_{Br}$ (sec)	$R_{Br,match}$ ( $\Omega$ )	
	50 Hz	60 Hz
1.5	18,000	7500
1.0	6900	3600
0.5	2180	1378
0.3	1100	755

power increases excessively.

Regarding the influence of the switching frequency of the inverter, despite the fact that its increase entails an increase in switching losses, it is observed not to adversely affect the energy fed into the electric brake. In contrast, increasing the switching frequency in the upper permissible values of 9 kHz and 12 kHz, increases substantially the said amount of energy. This is due firstly to the small size of switching losses compared to the inverter conduction and motor copper losses during braking (which increase proportionally to the square of the braking force). On the other hand the quality of the motor current waveform is improved by increasing the switching frequency—thereby reducing the proportion of copper loss associated with the skin effect. Finally, Figures 13-15 present indicative waveforms of the voltage at the brake resistance during braking.

#### 4.2. Section B: Laboratory Measurements with Load Dependent on the Square of the Angular Speed of Rotation

Experiment data:

- Total moment of inertia  $J_{ems} = 0.0140 \text{ kgm}^2$ .
- Mechanical load torque  $T'_L = 70\% - 100\%T_N$  (braking under high load).
- Frequency 50/60 Hz.
- Inverter switching frequency 6 kHz.
- Brake resistance 50  $\Omega$ .
- Free braking time 3.2 sec/1720 rpm, 2.0 sec/1439 rpm, 1.9 sec/1420 rpm.

Table 3 shows the matching resistance value for the three rotational speeds, according to Equation (17), taking into account the electrical losses of the electric motor system according to Figure 2.

As in Section A, the values in Table 3 it is evident that matching is achieved under extremely high values of the electric brake ohmic resistance, mainly due to the power level of the application. Therefore, in every case the ohmic resistance of the electric brake is less than the matching resistance. Hence, according to the theoretical analysis, the energy supplied to the brake resistance is expected to be greater than the recovered energy.

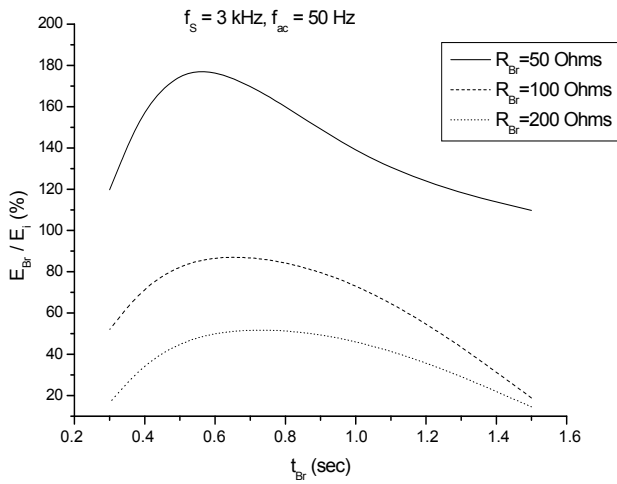


Figure 5. Energy recovery during Section A experimental process ( $f_s = 3 \text{ kHz}$ ,  $f_{ac} = 50 \text{ Hz}$ ,  $R_{Br}$  being parameter).

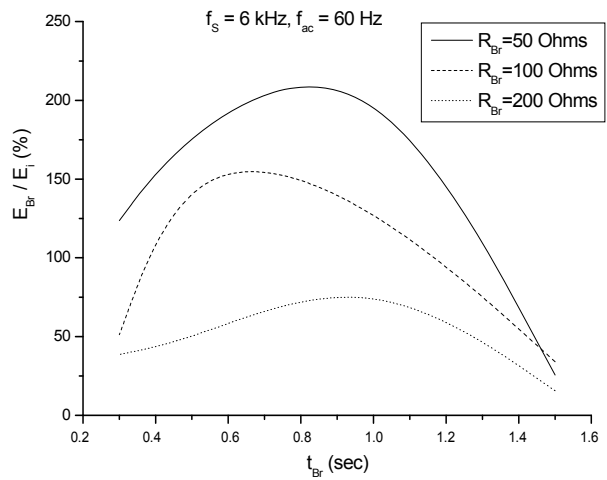


Figure 8. Energy recovery during Section A experimental process ( $f_s = 6 \text{ kHz}$ ,  $f_{ac} = 60 \text{ Hz}$ ,  $R_{Br}$  being parameter).

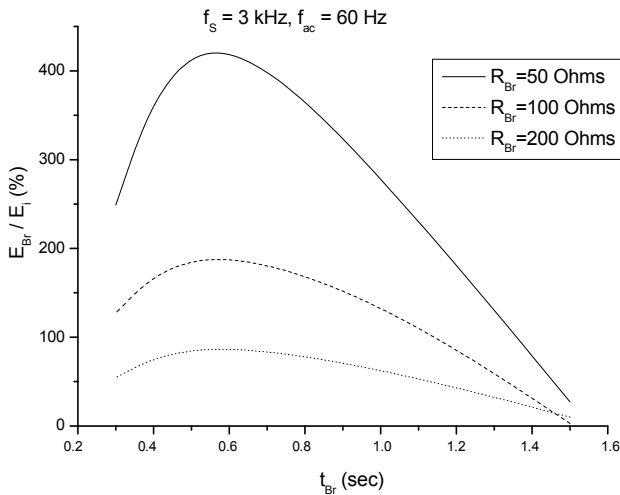


Figure 6. Energy recovery during Section A experimental process ( $f_s = 3 \text{ kHz}$ ,  $f_{ac} = 60 \text{ Hz}$ ,  $R_{Br}$  being parameter).

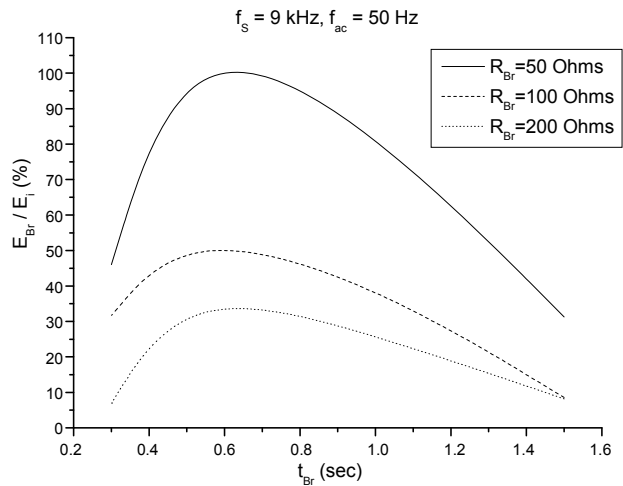


Figure 9. Energy recovery during Section A experimental process ( $f_s = 9 \text{ kHz}$ ,  $f_{ac} = 50 \text{ Hz}$ ,  $R_{Br}$  being parameter).

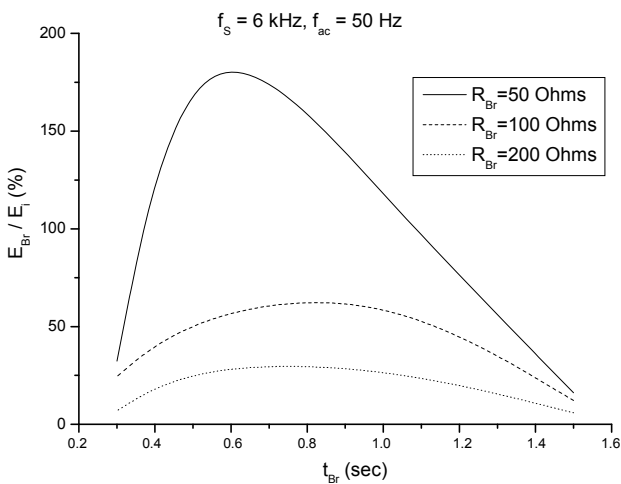


Figure 7. Energy recovery during Section A experimental process ( $f_s = 6 \text{ kHz}$ ,  $f_{ac} = 50 \text{ Hz}$ ,  $R_{Br}$  being parameter).

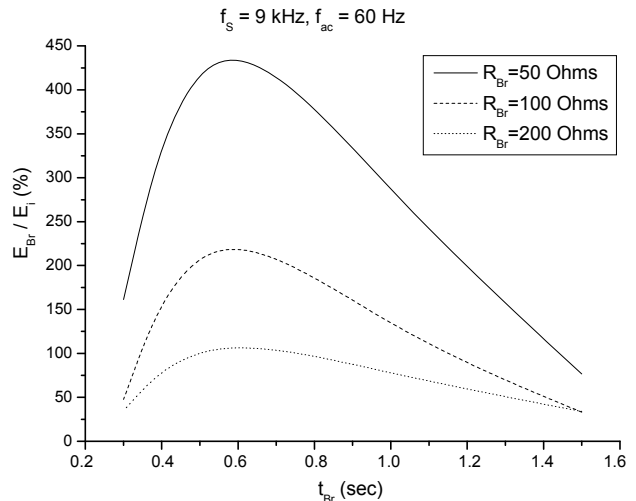


Figure 10. Energy recovery during Section A experimental process ( $f_s = 9 \text{ kHz}$ ,  $f_{ac} = 60 \text{ Hz}$ ,  $R_{Br}$  being parameter).

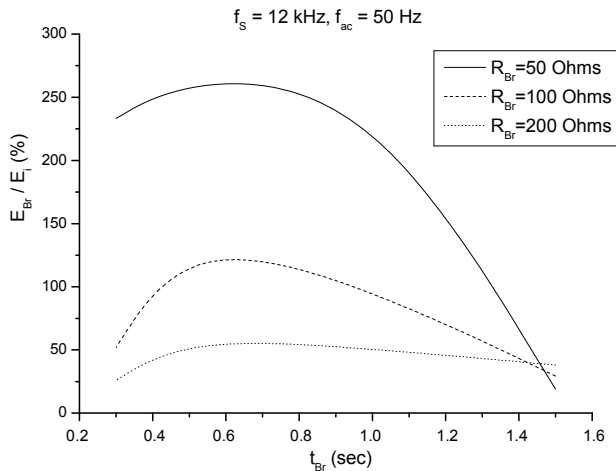


Figure 11. Energy recovery during Section A experimental process ( $f_s = 12$  kHz,  $f_{ac} = 50$  Hz,  $R_{Br}$  being parameter).

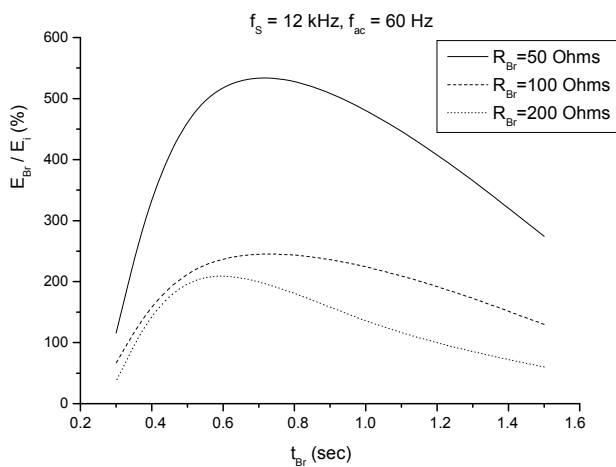


Figure 12. Energy recovery during Section A experimental process ( $f_s = 12$  kHz,  $f_{ac} = 60$  Hz,  $R_{Br}$  being parameter).

Table 3. Matching break resistor value for Section B experiments.

$t_{Br}$ (sec)	$R_{Br,match}$ ( $\Omega$ )		
	1439 rpm	1420 rpm	1720 rpm
1.5	11,700	134,900	5700
1.0	5530	11,478	2729
0.5	1705	2555	1077
0.3	882	1057	614

In the experimental results presented in Figure 16 it can be observed that the energy supplied to the resistance of the electric brake is extremely limited compared with Section A, because the high loading of the motor significantly reduces the free braking time and hence the potential energy recovery—as predicted by Equation (9). Additionally, a significant percentage of recovered energy is

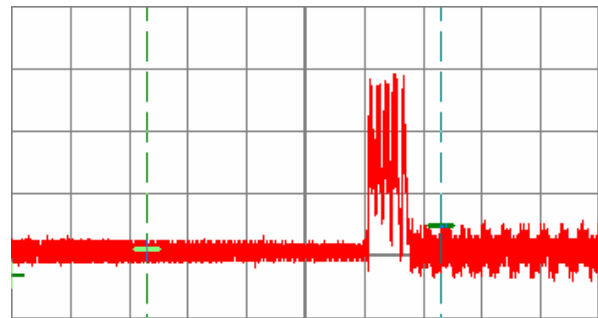


Figure 13. Brake resistor voltage waveform, (200 V/div, 1 sec/div, 50 Hz,  $f_s = 3$  kHz,  $R_{Br} = 50$  Ohm,  $t_{Br} = 0.5$  sec).

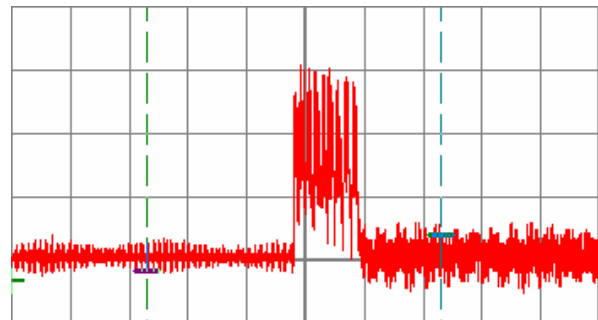


Figure 14. Brake resistor voltage waveform, (200 V/div, 1 sec/div, 60 Hz,  $f_s = 3$  kHz,  $R_{Br} = 50$  Ohm,  $t_{Br} = 0.5$  sec).

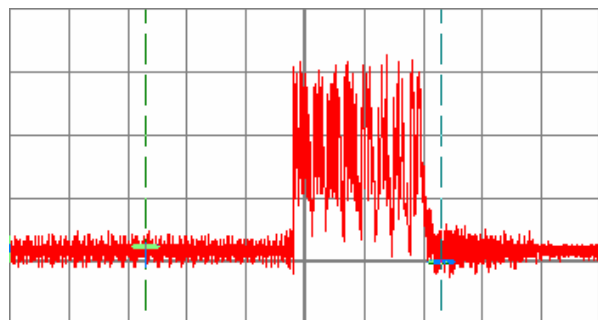


Figure 15. Brake resistor voltage waveform, (200 V/div, 0.5 sec/div, 60 Hz,  $f_s = 12$  kHz,  $R_{Br} = 50$  Ohm,  $t_{Br} = 0.5$  sec).

stored in the DC link capacitor, without creating a prohibitive overvoltage—due to the low braking power. Regardless of these observations, the energy reaching the brake can be in the order of 20% - 50%, suggesting a sizeable saving, particularly for industrial loads with frequent starts-stops. Finally, Figures 17 and 18 present indicative voltage waveforms in the brake resistance, during braking.

### 4.3. Discussion on the Experimental Outcomes

The experimental process has highlighted the fact that the regenerative braking application may be proven inefficient in cases that the braking resistor value is poorly set, as well as in cases that there is a braking semiconductor switch, consuming so excessive energy amounts.



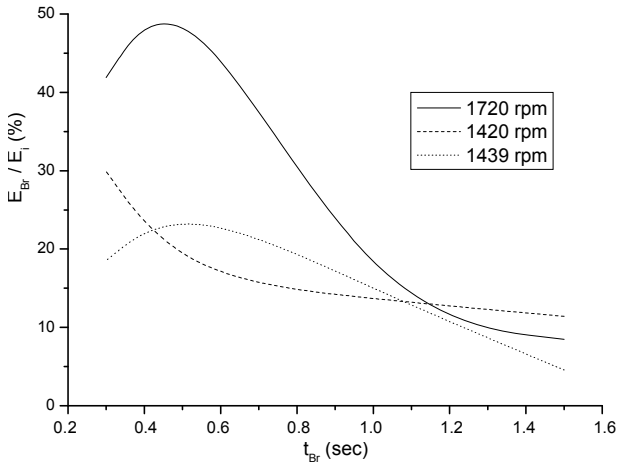


Figure 16. Energy recovery during Section B experimental process ( $f_s = 6$  kHz,  $R_{Br} = 50$  Ohm, rotor speed being parameter).

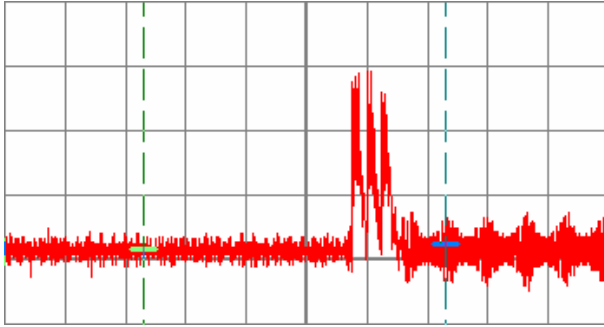


Figure 17. Brake resistor voltage waveform, (200 V/div, 0.5 sec/div, 1720 rpm,  $t_{Br} = 0.5$  sec).

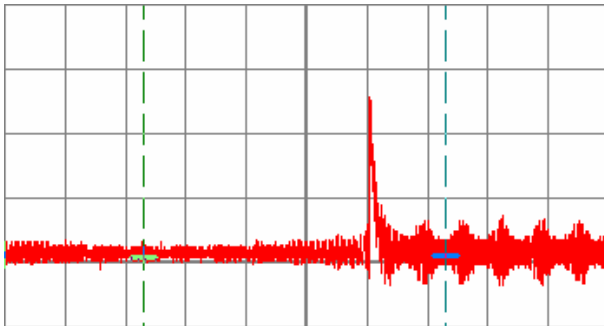


Figure 18. Brake resistor voltage waveform, (200 V/div, 0.5 sec/div, 1420 rpm,  $t_{Br} = 0.5$  sec).

For this reason, the operational aspects that the regenerative circuit must meet can be summarized to the following points:

- Operation during braking as a resistor;
- Automatic adjustment of the equivalent resistor value in order to be always in matched operation (absorbing only the regenerated energy amount);
- Fast control loop response so as to minimize the necessary time for the detection of the appropriate

- equivalent resistor value (matched operation);
- High efficiency under high braking torque conditions;
- Simple structure;
- Independent operation from the main motor driver topology.

### 5. The Proposed Power Converter for Braking Energy Exploitation

The proposed braking converter topology and its control concept are presented in **Figure 19**; the converter is connected directly to the DC link through a high frequency cut-off filter (due to the PWM operation) and it has the structure of a bidirectional buck/boost converter. In more details, when a braking interval occurs the DC link capacitor initially charges until the DC link voltage reaches its higher permissible value (which is set by the user). Then, a dc bus overvoltage signal is generated which enables the PWM operation of the semiconductor switch  $S_1$  while  $S_2$  is off ( $D_2$  operates as a freewheeling diode). Thus, the converter behaves as a buck charger, transferring energy to the storage unit (capacitor or supercapacitor bank in cases of higher power levels). If the DC link voltage drops below its low voltage value (which is also set by the user) then the charging operation stops. On the other hand, when the next operating cycle of the inverter starts the converter acts as a boost converter ( $S_1$  is off,  $S_2$  operates and  $D_1$  operates as a freewheeling diode), transferring the stored braking energy to the load. Finally, an emergency discharging branch is incorporated for protection against extreme voltage rise at the storage unit.

It is noted that the “Ohmic behavior” is achieved through the selection of the  $R_{Br}$  parameter in **Figure 19(b)**. Moreover, the converter in buck mode has to be designed in such a way, so as to reassure discontinuous conduction mode (DCM) for the  $L$ -inductor; as it is known [6], DCM operation produces the following relationship between the buck converter input voltage and current:

$$R_{in} = R_{Br} = \frac{V_{in}}{I_{in}} = \frac{2f_s L}{d^2(1-\lambda)} \tag{18}$$

- $R_{in}$ , the buck converter equivalent input resistance.
- $V_{in}$ ,  $I_{in}$ , the buck converter input voltage and current values.
- $d$ , the duty cycle of the PWM operation.
- $L$ , the inductor value.
- $f_s$ , the switching frequency of the PWM operation.
- $\lambda = \frac{V_o}{V_{in}} \leq 1$ , the input-output voltage ratio.

Thus, the DCM operation leads to an equivalent input resistance, representing the  $R_{Br}$  value, which depends on the output voltage ratio; according to Equation (18) the

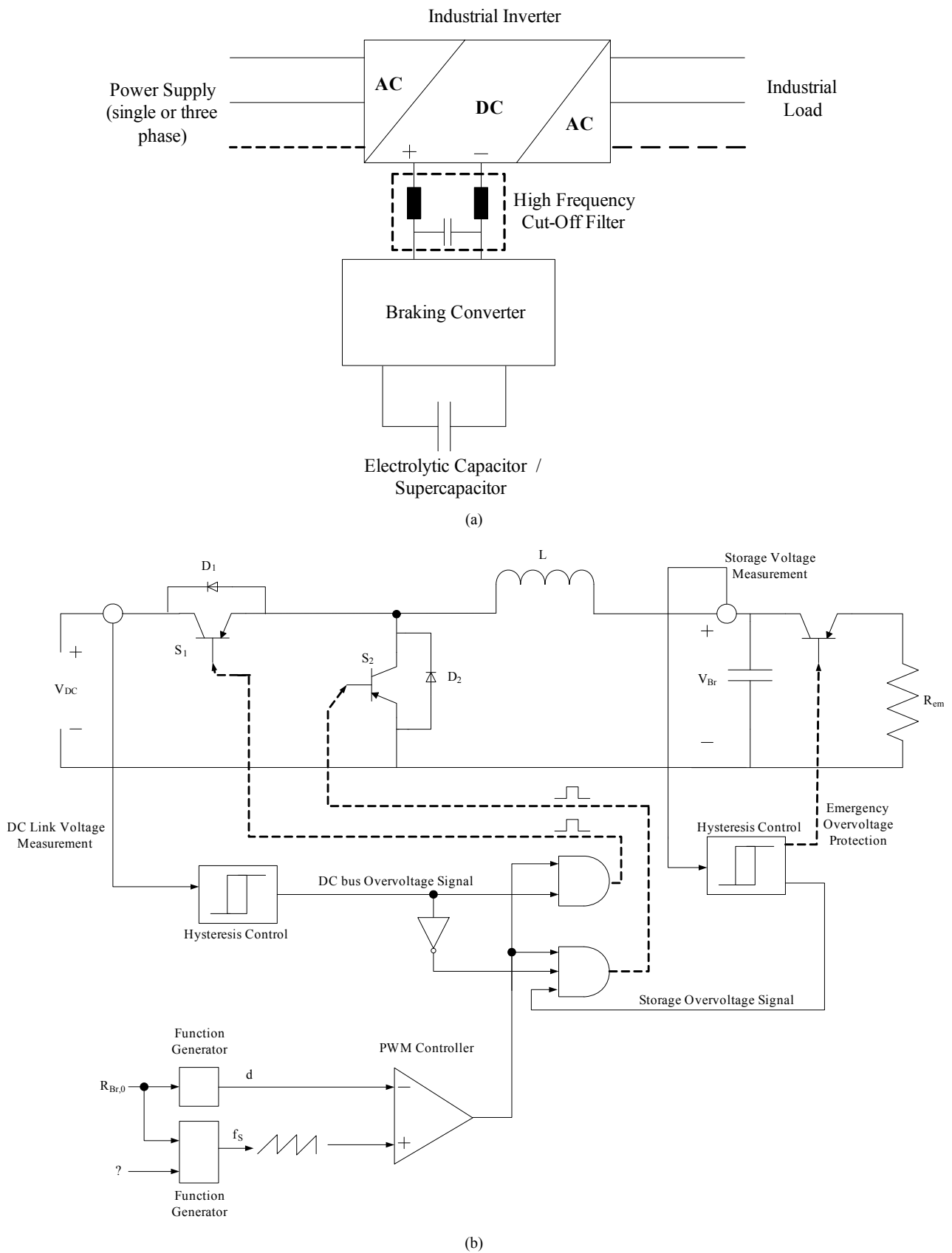


Figure 19. The proposed braking converter; (a) converter topology, (b) control concept.

$R_{Br}$  becomes constant if:

$$\frac{f_s}{f_{s,0}} = 1 - \lambda \quad (19)$$

$$R_{Br} = R_{Br,0} = \frac{2f_{s,0}L}{d^2} = \text{constant}$$

$f_{s,0}$ , the switching frequency for  $\lambda = 0 (V_o = 0)$

The control loop in **Figure 19(b)** keeps the  $R_{Br}$  value constant due to the voltage feedback, implementing so Equation (19). Moreover, the condition for DCM mode is [6]:

$$I_{in} \leq (1-d) \frac{V_{in}}{R_{in}} \quad (20)$$

Equation set (19), (20) can be used for the determination of  $L, f_{s,0}$  values so as to reassure DCM operation. As it concerns boost operation during discharge, this may be either CCM or DCM without any affection on the braking mode.

According to its operation description, the proposed regenerative converter manages to meet the requirements that have been set in the previous Section. In more details, the operation of the braking scheme is independent by the inverter topology and operation (it is connected directly to the DC bus), while it is a very simple structure. Finally, the fact that the braking energy is stored locally reduces the additional energy losses due to the energy injection to the grid.

## 6. MATLAB/Simulink Simulation Process

The proposed braking converter has been simulated in MATLAB/Simulink environment, for the case of the 2,5 kW system that has been experimentally studied. A typical acceleration—normal operation—braking operation cycle is presented in **Figure 20**—for the case of low load operation. The low and overvoltage thresholds for the DC link are set to 700 V and 750 V respectively (680 V nominal voltage during operation is supposed), while the equivalent resistance is set to 50 Ohm; a 1000  $\mu$ F capacitor has been used for the energy storage unit, with maximum permissible voltage fluctuation (during braking) is between 100 V - 600 V (175 Joule capacity while the initial kinetic energy of the rotating system is between 200 - 250 Joules, depending on the speed set). Finally, the industrial inverter switching frequency is 9 kHz. As it can be noted, the rotating speed increases/decreases linearly while the DC link voltage during braking has similar waveform with the ones that have been recorded during the experimental process.

A detailed simulation process took place in order to evaluate the operational characteristics of the proposed braking scheme for various values of the  $R_{Br}$  parameter. The outcomes are presented in **Figures 21-23**, in terms

of regenerative energy amount as a ratio of braking time and for  $R_{Br}$  being parameter. The theoretical calculation of the regenerative energy amount has been made by using Equation (15). Moreover, the simulation process has been performed each time for two alternative mains supply conditions; 1) the mains supply remains connected with the industrial inverter during braking, 2) the mains supply is disconnected by the industrial inverter during braking. The reason for this test is to quantify the excessive energy consumption during braking due to the mains supply presence.

The main outcome from the simulation results in **Figures 21-23** is that in case that the mains supply is disconnected during braking then the regenerative energy amount is very close to the expected theoretical one and it is almost independent by the selected  $R_{Br}$  value. Of course, higher  $R_{Br}$  values demand faster braking converter response (lower inductance values and higher switching frequencies) and so there is an upper limit. On the other hand, if the mains supply is connected during the braking interval there is notable excessive energy consumption by the braking unit—especially at higher  $R_{Br}$  and braking time values. This can be attributed to the fact that for such long braking intervals the rotating speed decrease diverges from the linear function that has been supposed during the theoretical analysis.

So, the main conclusion of the simulation procedure is that the braking unit optimum operation—in terms of energy exploitation—is achieved if the industrial inverter mains supply during braking is disconnected; this can be easily achieved if a triac bridge comes between the main supply and the industrial inverter. Thus, the firing signal of this bridge stops at the beginning of every braking interval, disconnecting so the inverter from the main power supply. This is a low cost solution that can be incorporated with minimum technical effort and for this reason it is considered to be effective.

## 7. Quantification of the Energy Recovery Potential for Industrial Loads

In the relevant literature [13-15] the quantification of energy recovery potential due to regenerative braking has been made only for electric vehicles. In the present work this quantification is made for the case of industrial loads, according to the theoretical analysis in Section 3, the simulation model that has been previously developed and for the main operation classes according to IEC 34-1. Obviously this work has many independent parameters and for this reason the present quantification is upon the following admissions:

- Average operating power 2.5 kW.
- 8000 h of operation per year.
- $t_{Br} = 0.5$  sec.

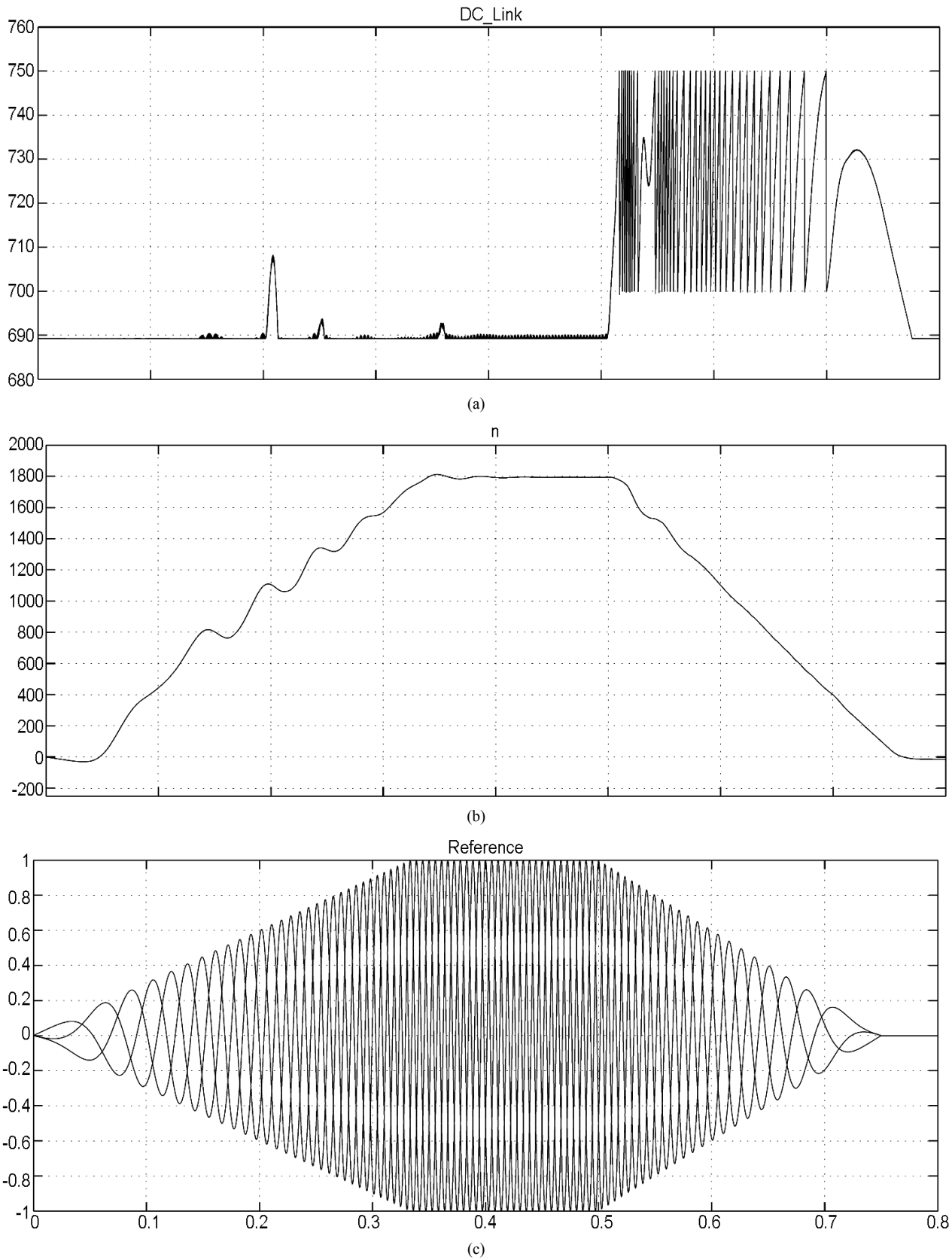


**Figure 20. Simulated waveforms during an operation cycle (acceleration-constant speed-braking); DC\_Link is the voltage on the DC bus, n (rpm) is the motor rotating speed, Reference is the SPWM control signals.**

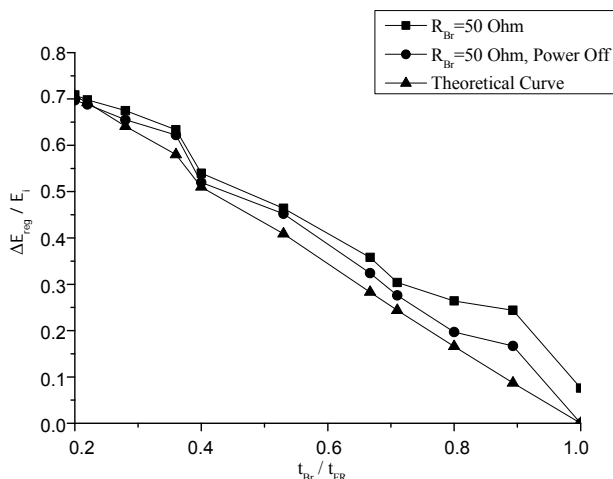


Figure 21. Simulation waveforms and the corresponding theoretical calculations for the regenerative energy amount as a function of braking time,  $R_{Br} = 50$  Ohm.

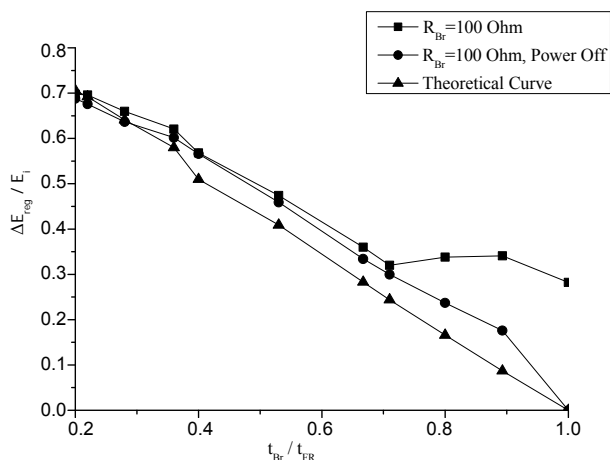


Figure 22. Simulation waveforms and the corresponding theoretical calculations for the regenerative energy amount as a function of braking time,  $R_{Br} = 100$  Ohm.

- The electric break always operates under matching conditions.
- The electric losses of the inverter-induction motor system are determined by its nominal efficiency,  $\eta_N$ , as:
  - $\eta_N = 75\%$ ,  $k = 8.5 \times 10^{-5} \text{ W}^{-1}$ ,  $P_o = 90 \text{ W}$
  - $\eta_N = 80\%$ ,  $k = 7.0 \times 10^{-5} \text{ W}^{-1}$ ,  $P_o = 70 \text{ W}$
  - $\eta_N = 85\%$ ,  $k = 5.8 \times 10^{-5} \text{ W}^{-1}$ ,  $P_o = 50 \text{ W}$

The energy saving,  $\frac{\Delta E_{sav}}{E_i}$ , can be calculated by the

formula:

$$\frac{\Delta E_{sav}}{E_i} = \frac{\Delta E_{reg}}{E_i} \cdot 8000h \cdot \frac{\text{brakes}}{h} \quad (21)$$

$\frac{\Delta E_{reg}}{E_i}$ , is calculated by Equation (15).

$\frac{\text{brakes}}{h}$ , are the average brakings per hour during a year of operation and they can be determined by the operation class

The energy amount (in kWh) that can be recovered on a year basis for the basic operation class  $S_1$  and for  $\frac{\text{brakes}}{h} = 1$ , is presented in **Figure 24** and it is an evident that the implementation of energy recovery for industrial loads may be beneficially. This remark is further reinforced by the calculation of energy saving amount as a ratio of the annual energy consumption for the most popular operation classes of industrial loads, according to the investigation in the Hellenic industry [1], shown in **Table 4**. It is worth mentioning that even for the

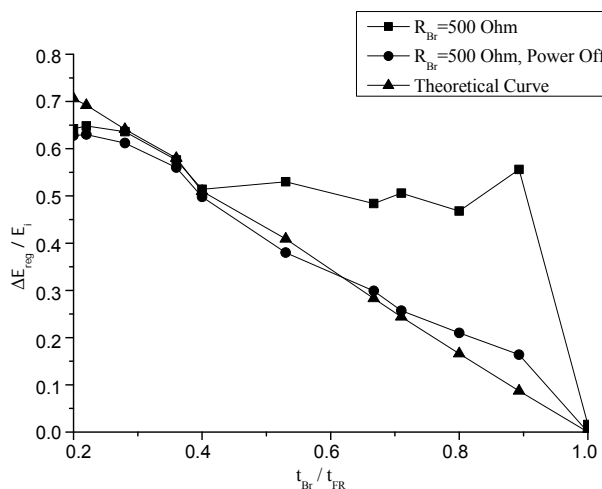


Figure 23. Simulation waveforms and the corresponding theoretical calculations for the regenerative energy amount as a function of braking time,  $R_{Br} = 500$  Ohm.

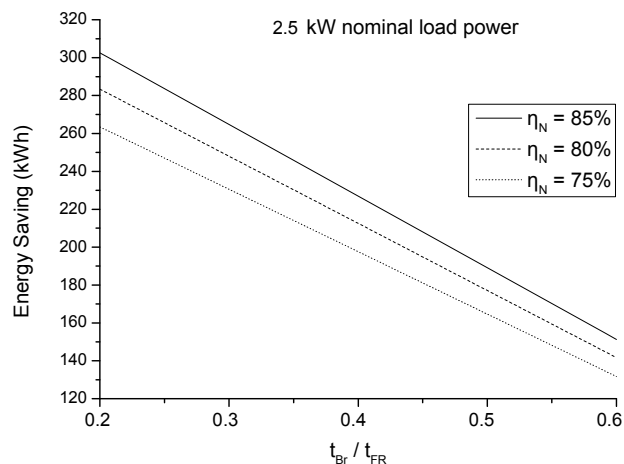


Figure 24. Energy saving calculation in industrial loads due to braking energy recovery, with the efficiency of the inverter-induction motor system being parameter.  $S_1$  operation class, one braking per hour.

**Table 4. Energy saving for various operation classes.**

Operation class according to IEC 34-1	brakes h	Annual Energy Saving (%)
S <sub>1</sub>	1 - 2	1.0% - 3.0%
	1	1.0% - 3.0%
S <sub>2</sub>	3	3.0% - 4.5%
	5	4.5% - 8.0%
	3	3.0% - 9.5%
S <sub>3</sub> , S <sub>4</sub>	7	6.0% - 16.0%
	10	8.5% - 18.0%
	3	5.0% - 9.5%
S <sub>5</sub>	7	8.5% - 18.0%
	10	11.0% - 20.0%

relatively small power level of 2.5 kW the expected energy saving can reach very satisfying levels—even more than 10%. This is a very important finding of the present work and it is comparable with the energy saving ratio that has been reported for electric vehicles [13-15]. Thus, the development of regenerative braking units dedicated for industrial loads is a very promising commercial sector.

Finally, the present energy saving calculation algorithm can be used for various power levels and operation classes of industrial loads, in order to assess whether the introduction of regenerative braking is cost effective or not.

## 8. Conclusions

The present paper investigated in detail both theoretically and experimentally the energy recovery potential in commercial inverters that drive industrial loads. The main conclusion from the results of this study is that energy recovery may vary at a satisfactory level (even higher than 10%), but require the proper design of the circuitry, which plays the role of brake resistance. Specifically, the energy recovery circuitry should act as a variable resistor, whose value will be set to the optimum value of the matching resistance. To achieve this goal, a braking converter topology and its control concept have been proposed and thoroughly studied through a detailed simulation process, proven to be very effective—in terms of energy regeneration—especially if the mains industrial inverter supply is disconnected during braking intervals.

Finally, as it concerns future work, the following options in this project should be studied further:

- The design and the implementation of the braking converter topology in form of parallel operating modules and the modification of its control loop in order to incorporate the interleaved pulse modulation. In this way the need for high frequency filtering will be

drastically reduced and the whole system will become a plug-n-play device of which power level can be increased or decreased just by adding or removing modules.

- The external setting of the equivalent resistance, entering data for the settable braking time, free braking time and the moment of inertia of the industrial load. In this way the optimum  $R_{Br}$  value can be calculated and set, cancelling so the need for a control loop that involves the DC link voltage (which in some types of inverters is not accessible but instead that a braking leg is available).

## 9. Acknowledgements

This work was supported by the “Reinforcement program of small and medium enterprises for research and technological development activities” under research project 23SMEs2009 and funded by the European social fund and by national funds.

## REFERENCES

- [1] N. Papanikolaou and Th. Ikonomakis, “Investigation of the Optimum Power Electronic Converter Topology for Reactive Power Compensation and Breaking Energy Exploitation for Industrial Processes,” 2012.
- [2] LG Inverters, Series iC5, iG5A, iS5, iP5A & iH, Technical Reference, 2012.  
[www.pconvent.ru/download/LG\\_iC5\\_Manual\\_ENG.pdf](http://www.pconvent.ru/download/LG_iC5_Manual_ENG.pdf)
- [3] AuCom Series EMX3, Technical Reference, 2012.  
[http://www.aucom.com/images/stories/aucom\\_resource\\_files/brochures/EMX3\\_Brochure.pdf](http://www.aucom.com/images/stories/aucom_resource_files/brochures/EMX3_Brochure.pdf)
- [4] Mitsubishi Inverters.  
[http://www.mitsubishi-automation.com/products/inverters\\_content.html](http://www.mitsubishi-automation.com/products/inverters_content.html)
- [5] R. Krishnan, “Electric Motor Drives: Modeling, Analysis, and Control,” Pearson Education, Inc., Prentice Hall, Upper Saddle River, 2001.
- [6] N. Mohan, T. Undeland and W. Robbins, “Power Electronics: Converters, Applications, and Design,” 2nd Edition, John Wiley & Sons Inc., Hoboken, 1995.
- [7] M. Rashid, “Power Electronics: Circuits, Devices and Applications,” Pearson/Prentice Hall, Upper Saddle River, 2003.
- [8] J. S. Jiang and J. Holtz, “An Efficient Braking Method for Controlled AC Drives with a Diode Rectifier Front End,” *IEEE Transactions on Industry Applications*, Vol. 37, No. 5, 2001, pp. 1299-1307. [doi:10.1109/28.952505](https://doi.org/10.1109/28.952505)
- [9] M. Rastogi and P. W. Hammond, “Dual-Frequency Braking in AC Drives,” *IEEE Transactions on Power Electronics*, Vol. 17, No. 6, 2002, pp. 1032-1040. [doi:10.1109/TPEL.2002.805613](https://doi.org/10.1109/TPEL.2002.805613)
- [10] P. J. Grbovic, P. Delarue, P. Le Moigne and P. Bartholomeus, “The Ultracapacitor-Based Regenerative Controlled Electric Drives with Power-Smoothing Capabil-

- ity,” *IEEE Transactions on Industrial Electronics*, Vol. 59, No. 12, 2012, pp. 4511-4522. [doi:10.1109/TIE.2011.2181129](https://doi.org/10.1109/TIE.2011.2181129)
- [11] S. Chapman, “Electric Machinery Fundamentals,” McGraw-Hill, New York, 2000.
- [12] G. Notton, V. Lazarov and L. Stoyanov, “Optimal Sizing of a Grid-Connected PV System for Various PV Module Technologies and Inclinations, Inverter Efficiency Characteristics and Locations,” *Renewable Energy*, Vol. 35, 2010, pp. 541-554. [doi:10.1016/j.renene.2009.07.013](https://doi.org/10.1016/j.renene.2009.07.013)
- [13] A. Adinolfi, R. Lamedica, C. Modesto, A. Prudenzi and S. Vimercati, “Experimental Assessment of Energy Saving Due to Trains Regenerative Braking in an Electrified Subway Line,” *IEEE Transactions on Power Delivery*, Vol. 13, No. 4, 1998, pp. 1536-1542. [doi:10.1109/61.714859](https://doi.org/10.1109/61.714859)
- [14] H. Seki, K. Ishihara and S. Tadakuma, “Novel Regenerative Braking Control of Electric Power-Assisted Wheelchair for Safety Downhill Road Driving,” *IEEE Transactions on Industrial Electronics*, Vol. 56, No. 5, 2009, pp. 1393-1400. [doi:10.1109/TIE.2009.2014747](https://doi.org/10.1109/TIE.2009.2014747)
- [15] M.-J. Yang, H.-L. Jhou, B.-Y. Ma and K.-K. Shyu, “A Cost-Effective Method of Electric Brake with Energy Regeneration for Electric Vehicles,” *IEEE Transactions on Industrial Electronics*, Vol. 56, No. 6, 2009, pp. 2203-2212. [doi:10.1109/TIE.2009.2015356](https://doi.org/10.1109/TIE.2009.2015356)